Title: Mathematical Modelling of Oxygenation Dynamics using High-Resolution Perfusion Data – Physiological Insights

Authors: Mansour T. A. Sharabiani, PhD[1†], Alireza S. Mahani, PhD[2†], Richard W. Issitt, DClinP[3,4,5], Yadav Srinivasan, MD[6], Serban Stoica, FRCS MD[7].

Affiliations:

1. School of Public Health, Imperial College, London, United Kingdom
2. Statman Solution Ltd., London, United Kingdom
3. Centre for Heart Failure, Transplantation and Extracorporeal Support, UCL Institute for Cardiovascular Science, UCL, London, United Kingdom
4. Perfusion Department, Great Ormond Street Hospital for Children, London, United Kingdom
5. Data Research, Innovation and Virtual Environments Unit, Great Ormond Street Hospital for Children, London, United Kingdom
6. Cardiac Surgery Department, Great Ormond Street Hospital for Children, London, United Kingdom
7. Cardiac Surgery Department, Bristol Royal Children's Hospital, Bristol, United Kingdom

† These authors contributed equally to this work.

Corresponding Author:

Dr Mansour T.A. Sharabiani
School of Public Health, Imperial College London
London, United Kingdom
Email: mt5605@imperial.ac.uk

Abstract

Background

Oxygen demand is a critical determinant of oxygen delivery levels in paediatric patients during surgeries and other clinical interventions. Current models, such as the van't Hoff equation, do not fully capture the complexities of oxygen demand as a function of temperature, age, and weight, particularly in diverse paediatric populations.

Objectives

The aim of this study is to quantify the relationships between oxygen demand and key physiological factors - including age, weight, and temperature - in paediatric patients, while testing the limitations of existing models. Additionally, we sought to explore the heterogeneity of oxygen extraction ratio (OER) response across age groups to changes in oxygenation parameters such as haemoglobin levels and arterial oxygen saturation.

Methods

We analysed data from a cohort of paediatric patients using an augmented version of the GARIX+ model, developed in Part 1 of this research. The augmented model incorporated age, weight and their interaction, as well as nonparametric temperature modelling via splines in a generalised additive models (GAM) framework. We also performed subgroup analysis by age to compare their dynamic OER response to changes in perfusion variables such as haemoglobin and arterial oxygen saturation.

Results

The augmented GARIX+ model demonstrated improved fit compared to baseline GARIX+. Oxygen demand per body surface area exhibited a non-linear relationship with age and weight, with the highest demand observed around 3 years of age. Oxygen demand shows positive correlation with weight in neonates and infants, and negative correlation in adolescents. The temperature dependence of oxygen demand indicated a more complex response than a constant Q_{10} assumption, with oxygen demand being less sensitive to mild hypothermia but becoming much more sensitive at deep hypothermia. Haemoglobin's impact on OER was found to be age-dependent, with younger patients displaying a diminished response.

Conclusions

This study provides new insights into the physiological determinants of oxygen demand in paediatric patients, emphasising the importance of age- and weight-specific models. The findings suggest that temperature dependence of resting metabolism is more complex than the constant-Q_{10} assumption of the prevailing van't Hoff model. These results underscore the need for personalized oxygen delivery strategies in paediatric care and challenge existing assumptions about oxygen demand in hypothermic conditions. Further validation in broader populations is recommended.

Keywords

cardiopulmonary bypass, van't Hoff, oxygen delivery, generalised additive models, system dynamics

Introduction

Oxygen demand is an important determinant of proper oxygen delivery – and minimisation of damage to vital organs – during cardiopulmonary bypass (CPB). However, predicting oxygen demand in real-time remains a challenge due to its complex

dependence on multiple physiological factors, including body temperature and patient characteristics.

In Part 1 of this research series [1], we used high-resolution data to develop the GARIX+ model to predict minute-by-minute changes in the oxygen extraction ratio (OER) during CPB surgeries in paediatric patients. This model successfully captured the slow, adaptive OER response to maintain oxygen consumption in line with oxygen demand as it fluctuates due to changes in body temperature during CPB.

In this paper, we study the physiological implications of our framework. To do so, we address two limitations of the baseline GARIX+ model introduced in Part 1. Firstly, while our data is limited to paediatric patients (18 years of age or younger), yet it covers a wide range of age groups, from neonates to adolescents, with potentially significant differences in their oxygenation physiology. To account for this heterogeneity in the data, we include terms representing the patient age and weight, as well as their interaction, in the steady-state component of the GARIX+ model to allow for variations in oxygen demand according to these two patient attributes. We also split the data into 4 age groups and compare the dynamic coefficients of the augmented GARIX+ models trained on the data restricted to each age group in order to identify heterogeneity of OER response by age.

Secondly, and following the prevailing literature as summarised in Kirklin and Blackstone (2012) [2] (hereafter referred to as KB12), in the baseline GARIX+ model we assumed that the dependence of oxygen demand on temperature follows the van't Hoff parametric form, where the logarithm of oxygen demand is a linear function of temperature. (The constant slope of the van't Hoff line translates to a constant Q_{10}, which is defined as the multiplicative increase in oxygen demand for every 10 degrees Celsius increase in body temperature.) However, evidence for this strong parametric assumption is scant. In fact, the Q_{10} estimated in KB12 is based on only two data points: a set of human experiments conducted at 20°C by Fox et al (1982) [3] (hereafter referred to as Fox82), and three sets of animal experiments conducted in the 1950s, at 37°C [4-6]. In this paper, we relax the van't Hoff assumption and allow the impact of temperature on oxygen demand to be revealed empirically from our data, using a nonparametric (spline) fit.

Finally, we show how the fitted GARIX+ model can simulate the Fox82 human experiments. In doing so, we illustrate how the hyperbolic form of the dependence of VO_2i (BSA-indexed oxygen consumption) on DO_2i (BSA-indexed oxygen delivery), fitted by Fox82 to the data, can emerge as a byproduct of a piecewise-linear model for asymptotic VO_2i, when subject to insufficient wait times between state transitions. We also illustrate how over-oxygenation can occur due to slowness of OER adaptations to changes in state variables such as cardiac flow.

This paper aims to provide a deeper understanding of the physiological determinants of oxygen demand in paediatric patients, offering a more nuanced model that accounts for key variables such as age, weight, and temperature. By doing so, we hope to contribute to the development of personalised oxygen delivery strategies during paediatric CPB.

For a list of nonstandard abbreviations and acronyms, see Supplementary Material A.

Methods

For Study Design and Participants, Data Collection, Anaesthesia and CPB, see Supplementary Material B.

Data Preparation

Data preparation and analysis were conducted using R 4.4.0, Python 3.11.7 and their various packages. For baseline data preparation, see Part 1 [1]. In addition to using age as a continuous variable, we also performed subgroup analysis by 'age group', using the following cutoffs: 'neonates': < 1 month; 'infants': between 1 month and 6 months; 'toddlers': 6 months to 3 years; 'children': > 3 years. Maximum age in our data is 18.23 years.

As in Part 1, we used the AKI score - defined for each operation according to KDIGO - to restrict our GARIX+ model to data points coming from operations with AKI=0 postoperatively. This means that the physiological insights generated by the model are based on AKI-free patients, rather than reflecting potential pathological changes in patients who ultimately suffered from AKI.

Baseline GARIX+

Minute-by-minute changes to logit of OER are assumed to be i.i.d. draws from a normal distribution. The mean of this normal distribution is the sum of three term groups: an equilibrium term group (ETG), an autoregressive term group (ATG) and an exogenous term group (XTG). ETG reflects a corrective force on OER that is proportional to the difference between the oxygen demand and oxygen consumption at any time. ATG and XTG reflect the effect on OER of past changes in the endogenous variable (OER) as well as the intended and past changes in the exogenous variables (T, CI, Hb and SaO_2). The number of lag terms (n) is a hyperparameter of GARIX+. In Part 1, we showed that $n = 7$ is sufficient. Unless said otherwise, in this paper we will be using GARIX+(7) and simply refer to it as GARIX+.

Augmented GARIX+

In the baseline GARIX+, ETG is given by:

$$ETG = \eta_0 \log(VO_2i)_t + \eta_1 + \eta_2 T_t, \quad (1)$$

where η_0, η_1 and η_2 are coefficients estimated during GARIX+ training. In the 'augmented' GARIX+, we include terms for patient age, weight (and their interaction) and modify the temperature dependence from linear to a nonparametric spline:

$$ETG = \eta_0 \log(VO_2i)_t + \eta_1 + \eta_2 s(T_t, 2) + \eta_3\, Age + \eta_4\, Weight + \eta_5\, Age \times Weight \quad (2)$$

Recall from Part 1 that in steady state – when oxygen consumption equals oxygen demand, OER and all other state variables do not change over time, and hence we must have $ETG = 0$. This implies the following expression for oxygen demand (or target oxygen consumption, tVO_2i):

$$\log(tVO_2i) = \alpha_0 + \alpha_1\, s(T, 2) + \alpha_2\, Age + \alpha_3\, Weight + \alpha_4\, Age \times Weight \quad (3)$$

where $\alpha_n = -\frac{\eta_{n+1}}{\eta_0}, n = 0,1,2,3,4$.

Q_{10} is calculated using the following equation:

$$Q_{10}(T) = \exp\left(10 \frac{\partial \log tVO_2i(T)}{\partial T}\right) \quad (4)$$

Under van't Hoff specification, the partial derivative and hence Q_{10} are constant, i.e., independent of temperature (T). We used a finite-difference approximation to Equation 4 for calculating and plotting Q_{10} as a function of T.

Comparison to Schofield

Predictions of the Schofield equations for the Basal Metabolic Rate (BMR) of each child were used as a reference for comparing the augmented GARIX+ predictions. These equations use age, weight, and sex of the child and are widely adopted for assessing energy expenditure in paediatric populations and are recommended by the World Health Organization (WHO) for international use. The following provides BMR in kcal/day as a function of age (years) and weight (kg) for each gender:

Boys:

0 < age < 3 ➔ 59.512 × W - 30.4

3 < age < 10 ➔ 22.706 × W + 504.3

10 < age < 18 ➔ 17.686 × W + 658.2

Girls:

0 < age < 3 ➔ 58.317 × W - 31.1

3 < age < 10 ➔ 20.315 × W + 485.9

10 < age < 18 ➔ 13.384 × W + 692.6

Results

Patients and Outcomes

Table 1 shows a summary of patients used in the study and their outcomes. The observed 30-day mortality rate was below the expected mortality rate - for the same operations - calculated according to the PRAiS2 protocol [7]. Most patients were under 1-year-old (neonates and infants: 54%) and did not have an antenatal diagnosis (57%).

Baseline vs. Augmented GARIX+

While the terms corresponding to the logarithm of age and weight alone do not have statistical significance, their interaction does, with a coefficient of -2.33 x 10^{-3} (or equivalently, -5.5 x 10^{-2} for predicting the logarithm of VO_2i) and p-value of 0.008. The ANOVA test for the spline term for temperature is also significant (p-value of 6.4 x 10^{-11}).

All likelihood-ratio tests comparing the baseline GARIX+, the augmented GARIX+ as well as the intermediate steps from baseline to augmented model produced statistical significance for improvements (adding age and weight, or changing the dependence on temperature from linear to nonparametric), with all p-values being less than 0.001.

Comparison to Schofield

Figure 1 shows a comparison of Basal Metabolic Rate (BMR) per kilogram of weight as a function of age, as implied by the oxygen-demand prediction of the baseline and augmented GARIX+ models, against the Schofield equations [8]. We see that the augmented GARIX+ model matches the Schofield equations more closely, both in absolute values and in consistency of shape (as quantified by the standard deviation of the differences on the log scale). In particular, we note that the BMR per kilogram predicted by the baseline GARIX+ is purely driven by the BSA factor, since in this model tVO_2i has no explicit dependence on age or weight. In contrast, and after adding logarithm of age and weight as well as their interactions, the BMR predictions reflect the trend in Schofield, i.e., modest increase in BMR from birth to about 3 years of age, followed by a steep decline afterwards.

Oxygen Demand vs. Patient Age and Weight

Figure 2A shows a 3D plot of the predicted (BSA-indexed) oxygen demand as a function of age and weight, using all unique combinations of (age, weight) from the training data. At young ages, weight is positively correlated with oxygen demand, while this relationship weakens and eventually reverses at older ages. This is due to the negative coefficient for the interaction term between age and weight in the augmented GARIX+

model, and can be seen more clearly in panel B which shows the dependence of oxygen demand on weight at four different ages, each representative of an age group. For instance, a 10% increase in the weight of a 5-day-old neonate above average would lead to a 2% 'increase' in oxygen demand (per BSA), while a 10% increase in the weight of an 8-year-old child above average would produce a 1% 'decrease' in oxygen demand.

Panels C and D show the projection of data in Panel A onto weight vs. oxygen demand plane, and age vs. oxygen demand plane, respectively. In both cases, we see that oxygen demand increases as the child becomes older (and heavier) but it reaches a peak of 85 mL/min/m2 at 3 years of age (at which point the child weights ~13 kilograms on average). Meanwhile, oxygen demand is as low as 47 and 70 mL/min/m2 in neonates and teenage children (of average weight), respectively.

OER Dynamics by Age Group

Figure 3 shows the coefficients of exogenous term groups corresponding to the haemoglobin ($\log Hb$) and arterial oxygen saturation ($\log SaO_2$) as a function of term lag (n), and where data is split by age group of patients. For $\log Hb$, we see a clear trend where the coefficients become smaller in magnitude as we approach younger ages. In other words, in neonates and infants the OER adaptation to haemoglobin changes is much less pronounced compared to older children. For $\log SaO_2$, we see the opposite where neonates and infants show a more pronounced immediate response in OER to a change in SaO_2.

Supplementary Material C shows similar plots for other state variables, also stratified by age group, where no clear trends by age group can be discerned.

Oxygen Demand vs. Temperature

Figure 4A shows oxygen demand vs. temperature, averaged – geometrically – over all unique (age, weight) combinations in the data. Panel B shows Q_{10} as a function of temperature, averaged arithmetically over the data. It starts at 3.8 at 16C, falling gradually to 3.6 at 25C before rapidly declining to 1.1 at 35C. Put differently, the first 5-degree reduction in body temperature from 36.8C to 31.8C only produces an 11% reduction in oxygen demand, while the next 5 degrees lead to a much more pronounced reduction of 37% in oxygen demand. In contrast, the constant Q_{10} of 2.2 produced by the baseline GARIX+ (dashed red line in Figure 3B) would predict a 33% reduction in oxygen demand for every 5 degrees reduction in body temperature throughout the cooling process.

Note that the wider confidence intervals at low temperatures are due to high concentration of data points in the high-temperature regime. For instance, only 4% of our intraoperative data points have temperatures below 25C.

GARIX+ vs. Fox82

We used the baseline GARIX+ model (see Part 1) to closely simulate the human experiments of Fox82 (Supp Mat C). A critical parameter is the wait time between step-function changes in cardiac index, which is 10 minutes in Fox82. As Figure 5 shows, the GARIX+ results (VO_2i vs. CI scatterplot) resemble the experimental data of Fox82. This notion is formalised in Table 2, which compares the hyperbolic fit of Fox82 against our hyperbolic fit to GARIX+ simulations: For all three parameters, our 95% confidence intervals cover the values reported by Fox82.

Recalling from Part 1, however, that the timescale of adaptations predicted by GARIX+ is significantly longer than 10 minutes, we perform a second experiment where we increase the wait time between CI step changes from 10 to 100 minutes. Figure 1 shows the resulting data points and the hyperbolic fit, which is now closer to the underlying piecewise linear assumption of GARIX+. As we increase the wait time further, the piecewise linear form is reconstructed asymptotically.

KB12 combine the Fox82 human experiments conducted at 20C with animal experiments done in the 1950s [4-6] at 37C. Using these two sets of experiments, and assuming a linear dependence of the logarithm of oxygen demand on temperature (the van't Hoff model), KB12 interpolate to predict an asymptotic oxygen consumption for all temperatures [2]. These number are shown in the 'Kirklin – Asymptotic' column of Table 3. KB12 also provide clinical recommendations for cardiac index and the expected VO_2i values, with the latter shown in the 'Kirklin – Clinical' column. We have also included in Table 3 the augmented GARIX+(7) predictions for oxygen demand (tVO_2i) for the same temperatures and evaluated at 4 representative ages (and their corresponding average weights), as well as the corresponding minimum oxygen delivery needed to satisfy the demand, assuming maximum OER values of 50% and 20%.

Note that GARIX+ and KB12 figures are not directly comparable for two reasons. Firstly, the human subjects used in Fox82 to collect the data at 20C were much older (57 +/- 10 years) than our paediatric patients. Secondly, the high-temperature leg of the data used by KB12 are all based on animal – rather than human – experiments. With these caveats in mind, we note that GARIX+ predictions are close to the 'Kirklin - Clinical' values at 20C, with the two diverging at higher temperatures, where KB12 implies higher oxygen demand than GARIX+.

Short-Term vs. Long-Term Oxygenation Gap

The classic view holds that the body extracts the oxygen it needs if supply is sufficient. As such, a static interpretation of the piecewise linear model only allows for the possibility of under-oxygenation. A dynamic interpretation, however, permits over-oxygenation in the near term. Figure 6 shows simulation results using the baseline GARIX+ model for oxygenation gap (OG) as a function of percent change in supplied oxygen at t=0 and time elapsed since supply change. OG is defined as the % difference between oxygen consumption at time t (VO_2i_t), and target oxygen consumption (tVO_2i): $OG_t = 100 \times (VO_2i_t - tVO_2i)\ /\ tVO_2i$. (Note that tVO_2i does not change over time since temperature is fixed).

The simulations demonstrate that, for small t's, the response is nearly linear, corresponding to relatively little adaptation in OER. The interpretation is that, e.g., when cardiac index is increased and before OER adaptively decreases to bring VO_2i down to its pre-perturbation level, there will be a nearly proportional oxygen consumption surplus, or over-oxygenation. However, as time progresses, such oxygen surplus dissipates as OER adaptively decreases. While oxygen surplus eventually vanishes, oxygen deficit cannot completely disappear if the ratio tVO_2i/DO_2i implies an OER greater than 1 (or perhaps a lower, physiologically plausible upper bound on OER). As a result, the piecewise linear shape emerges for very large t's.

Discussion

Oxygen Demand vs. Age and Weight

In this study, we utilised the GARIX+ model to quantify the relationship between oxygen demand and two critical patient attributes: age and weight. Our findings demonstrate a clear non-linear relationship, where oxygen demand per unit body surface area (BSA) increases as the child gets older, but peaks around 3 years of age, before tapering off at older ages. Similarly, when expressed in BMR per kilogram, the augmented GARIX+ model closely reproduced the Schofield curve for children. While the latter is discontinuous due to use of different equations in sub-intervals of 0-18, the GARIX+ curve is smooth (Figure 1), and perhaps more physiologically plausible. These insights could help clinicians better anticipate metabolic demands during surgeries and optimize oxygen delivery strategies accordingly.

Our observation of non-linear relationship between oxygen demand per kilogram and age in children, consistent with the Schofield curve, reflects the dynamic changes in growth and metabolism during childhood. Oxygen demand increases as children grow due to rapid cellular and organ development, peaking around age 3 when growth rates are high. After age 3, as growth slows and body composition stabilizes, oxygen demand

per kilogram begins to taper off. This decrease continues into adolescence as children's bodies require less relative oxygen for maintenance, reflecting a natural adjustment in metabolism with age. Therefore, our observation reinforces the importance of individualizing oxygen delivery based on age and weight rather than a one-size-fits-all approach.

We also reported a progressively weaker haemoglobin response in younger patients. During CPB, other than through hemofiltration, the only way to increase Hb concentration is through the addition of stored red blood cells (RBCs). Due to the large volume of the CPB circuit relative to the child's circulating volume, RBC transfusions are more common in paediatric than adult surgery. A recent study examined the effect of RBC transfusion on renal oxygenation in kidneys supported via an ex vivo normothermic kidney perfusion rig [8]. It demonstrated that there was slower O_2 unloading from stored RBC with concomitant reduction in O_2 extraction in perfused kidneys, indicating diffusion-limited O2 release at capillaries. It is also possible that SaO_2 dependence on PaO_2 - i.e., the oxygen dissociation curve - shifts differently with transfused RBC's due to the metabolic and morphological changes that can occur due to storage [9,10].

Dependence of Q10 on Temperature Regime

Oxygen can regulate glycolysis via the Pasteur effect. The availability of oxygen will suppress glycolysis, and decreased availability leads to an acceleration of glycolysis, at least initially. This appears to be regulated by several factors including the allosteric regulators of glycolysis (enzymes such as hexokinase) [11].

Allosteric enzymes do not follow the van't Hoff dependence on temperature, instead often displaying a sigmoid shape for dependence of reaction velocity on temperature, at a fixed substrate concentration.

Whilst Q_{10} has been traditionally used to describe the dependence of rate of chemical reactions on temperature, enzymatic reactions have ranges over which the proteins can operate before conformational changes or denaturing occurs. Furthermore, bypass physiology is very different from normal human physiology, in that exogenous variables (such as haemoglobin concentration, cardiac index etc.) are manipulated separately by the perfusionist, rather than in coordination, as would be under normal biology. For instance, normal physiological mechanisms to combat hypothermia (such as shivering) are prevented through general anaesthesia, and PaO_2 is managed at levels higher than observed naturally, to allow a margin of safety. Our nonparametric formulation, in the augmented GARIX+, of oxygen demand vs. temperature revealed that Q_{10} is significantly lower at higher temperatures, dropping from 3.8 at 16C to a mere 1.2 at 37C. One might postulate that under mild hypothermic conditions sufficient substrate (in

terms of CI and therefore energy) and oxygen is being provided, and enzymatic functions are maintained such that they lead to a degree of decoupling between metabolic rate and temperature. On cooling further into moderate and then deep hypothermia, this independence is lost, and higher Q_{10} values are observed as a result. However, further independent data are required to validate these observations, and experimentation is needed to determine the cellular mechanisms operating in different temperature regimes.

Limitations and Future Directions

Despite the robustness of our model, there are limitations that need to be acknowledged. First, our study cohort comprises only paediatric patients, which may limit the generalizability of our findings to adult populations. Furthermore, while our model captures a wide range of physiological responses, it does not account for all possible patient-specific variables, such as genetic factors or comorbidities. Additionally, the low-temperature data points are sparse, which limits our ability to make definitive conclusions about oxygen demand at extreme hypothermic conditions. Future studies should seek to validate these results in larger, more diverse cohorts and further explore the mechanistic underpinnings of temperature-oxygen demand relationships.

Conclusions

This study provides novel insights into the physiological determinants of oxygen demand in paediatric patients, with a particular focus on age, weight, and temperature modulation. By augmenting the baseline GARIX+ model and incorporating nonparametric temperature-dependence through spline modelling, we have demonstrated that oxygen demand is both non-linear and highly dependent on patient-specific factors. The relationship between oxygen extraction ratio (OER) and haemoglobin, as well as arterial oxygen saturation, underscores the need for tailored approaches to oxygen delivery, particularly in neonates and infants, where physiological responses differ significantly from older children.

The findings from this study challenge conventional assumptions, such as the fixed Q10 relationship, and highlight the importance of adaptive models in optimizing clinical decision-making, especially in complex settings like cardiopulmonary bypass. While this research offers important contributions, it also opens the door for further exploration, particularly in validating these findings across more diverse populations and refining strategies for oxygen demand management in extreme thermal conditions.

Future work should aim to expand these models to adult cohorts and explore the interaction between other physiological variables and oxygen demand. Ultimately, this

work lays a foundation for more personalized and precise management of oxygenation in paediatric care, which could lead to improved outcomes in critical clinical settings.

Funding

This work was (partly) funded by the National Institute for Health Research Great Ormond Street Hospital Biomedical Research Centre. The views expressed are those of the author(s) and not necessarily those of the National Health Service, the National Institute for Health Research, or the Department of Health.

Disclosures

Authors have no disclosures.

References

1. Sharabiani, Mansour Taghavi Azar, et al. "A Dynamic Time-Series Model of Oxygen Consumption during Paediatric Cardiopulmonary Bypass." medRxiv (2024): 2024-03.
2. Kirklin, James K., and Eugene H. Blackstone. Kirklin/Barratt-Boyes Cardiac Surgery: Expert Consult-Online and Print (2-Volume Set). Elsevier Health Sciences, 2012.
3. Fox, Lawrence S., et al. "Relationship of whole body oxygen consumption to perfusion flow rate during hypothermic cardiopulmonary bypass." The Journal of Thoracic and Cardiovascular Surgery 83.2 (1982): 239-248.
4. Cheng, Huan-Chen, et al. "A study of oxygen consumption during extracorporeal circulation." ASAIO Journal 5.1 (1959): 273-278.
5. Paneth, Matthias, et al. "Physiologic studies upon prolonged cardiopulmonary bypass with the pump-oxygenator with particular reference to (1) acid-base balance,(2) siphon caval drainage." Journal of Thoracic Surgery 34.5 (1957): 570-579.
6. Starr, Albert. "Oxygen consumption during cardiopulmonary bypass." The Journal of Thoracic and Cardiovascular Surgery 38.1 (1959): 46-56.
7. Rogers, Libby, et al. "Improving risk adjustment for mortality after pediatric cardiac surgery: the UK PRAiS2 model." The Annals of thoracic surgery 104.1 (2017): 211-219.
8. Schofield, William N. "Predicting basal metabolic rate, new standards and review of previous work." Human nutrition. Clinical nutrition 39 (1985): 5-41.
9. Khwaja A. KDIGO clinical practice guidelines for acute kidney injury. Nephron Clin Pract 2012;120:c179-184. doi: 10.1159/000339789

10. Naik SK, Elliott MJ. Ultrafiltration and paediatric cardiopulmonary bypass. Perfusion 1993;8:101-112. doi: 10.1177/026765919300800114
11. Dumbill R, Rabcuka J, Fallon J, et al. Impaired O2 unloading from stored blood results in diffusion-limited O2 release at tissues: evidence from human kidneys. Blood 2024;143:721-733. doi: 10.1182/blood.2023022385
12. Bennett-Guerrero E, Veldman TH, Doctor A, et al. Evolution of adverse changes in stored RBCs. Proc Natl Acad Sci U S A 2007;104:17063-17068. doi: 10.1073/pnas.0708160104
13. Yoshida T, Prudent M, D'Alessandro A. Red blood cell storage lesion: causes and potential clinical consequences. Blood Transfus 2019;17:27-52. doi: 10.2450/2019.0217-18
14. Lenzen S. A fresh view of glycolysis and glucokinase regulation: history and current status. J Biol Chem 2014;289:12189-12194. doi: 10.1074/jbc.R114.557314

Tables

Table 1: Patients and Outcomes

Variable	**Value**
Number of operations/patients	963/879
Median age at operation (months)	8.9 [3.1-48.7]
Range	0-218.8
Age group (at operation)	
Neonates (0-30 days)	148 (15)
Infants (1-6 months)	377 (39)
Toddlers (6 months -3 years)	152 (16)

Children (3-18 years)	286 (30)
Gender	
Male	481 (55)
Female	398 (45)
Ethnicity	
White	430 (49)
BAME	327 (37)
<Not Available>	122 (14)
Antenatal diagnosis	
Yes	360 (37)
No	548 (57)
<Not Available>	55 (6)
30-day mortality	
Expected (using PRAiS)	14 (1.6)
Observed	2 (0.2)

Table 1: Summary of patients and their outcomes. Numbers in brackets represent interquartile ranges for numeric variables, while numbers in parentheses represent

percentages for discrete variables. For gender and ethnicity, the counts and percentages are reported at the patient level, while for other variables (including age), the figures are reported at the operation level. For 30-day mortality, all calculations are based on a subset of 882 operations (827 patients) for which PRAiS2 score, discharge date and discharge status were available. Percentages may not add up to 100 due to rounding. BAME: Black, Asian and Minority Ethnic.

Table 2: GARIX+ vs. Fox82 – Hyperbolic Parameters

	GARIX+(7)		**Fox82**
Parameter	**estimate**	**95% CI**	**estimate**
R-squared	72.1%	48.4% - 92.9%	65%
a	30.8	21.3 – 46.6	35
b	0.84	0.39 - 1.54	0.42

Table 2: Comparison of R-squared and fit parameters from GARIX+(7) simulations mimicking experiments of Fox82 [2]. See Supp Mat B for model specification in Fox82 and their definitions of ‘a’ and ‘b’. Confidence intervals are based on 100 runs.

Table 3: GARIX+ vs. Kirklin – Oxygen Demand and Temperature

Temp (C)	**Kirklin**		**GARIX+ - Baseline**	**GARIX+ - Augmented**			
	Asymptotic	**Clinical**		**neonate (5-days)**	**infant (3-month)**	**toddler (1-year)**	**child (8-years)**
15	23	NA	18	12	18	21	19
20	35	27	26	17	26	30	27
25	55	42	36	24	38	43	38
30	86	65	51	34	54	62	55
37	161	120	83	57	89	102	90

Table 3: Comparison of Kirklin and GARIX+ predictions for oxygen demand at different temperatures. ‘Kirklin – Asymptotic’ corresponds to oxygen consumption at infinite cardiac index using the hyperbolic model fit to human and animal experiments. ‘Kirklin – Clinical’ values are taken from Kirklin et al (2012) textbook, Figure 2-11 (‘X’ marks). ‘GARIX+ - Naïve’ are steady-state prediction of the baseline GARIX+(7) model without the age and weight terms and without temperature nonlinearity. ‘GARIX+ - Augmented’ columns show steady-state oxygen demand predictions from a GARIX+(7) model that includes age, weight and their interaction (but no temperature nonlinearity).

Figures

Figure 1. Basal Metabolic Rate vs. Age

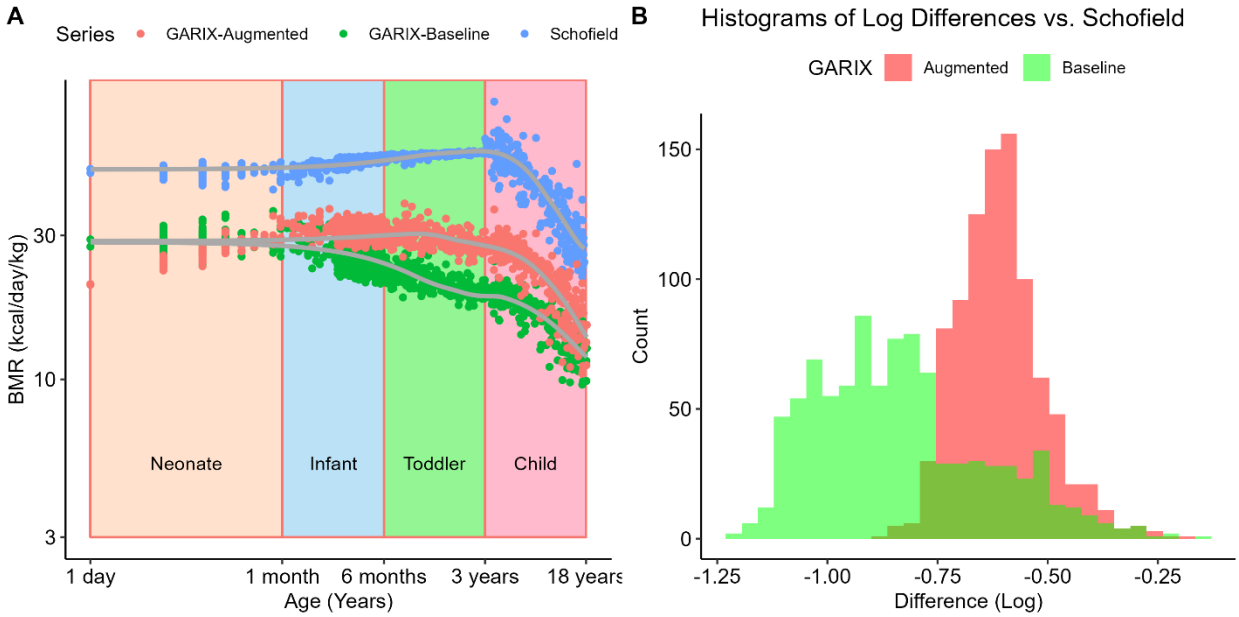

Figure 1: A) Comparison of predicted BMR vs. Age between Schofield, baseline GARIX+ and augmented GARIX+. Each data point corresponds to a patient in our dataset. LOESS fits to each dataset are overlaid as grey curves. Note that x and y axes are displayed in log scale. B) Histogram of differences in log of baseline and augmented GARIX+ vs. Schofield (Wilcoxon test p-value < 2.2e-16).

Figure 2. Oxygen Demand vs. Patient Age and Weight

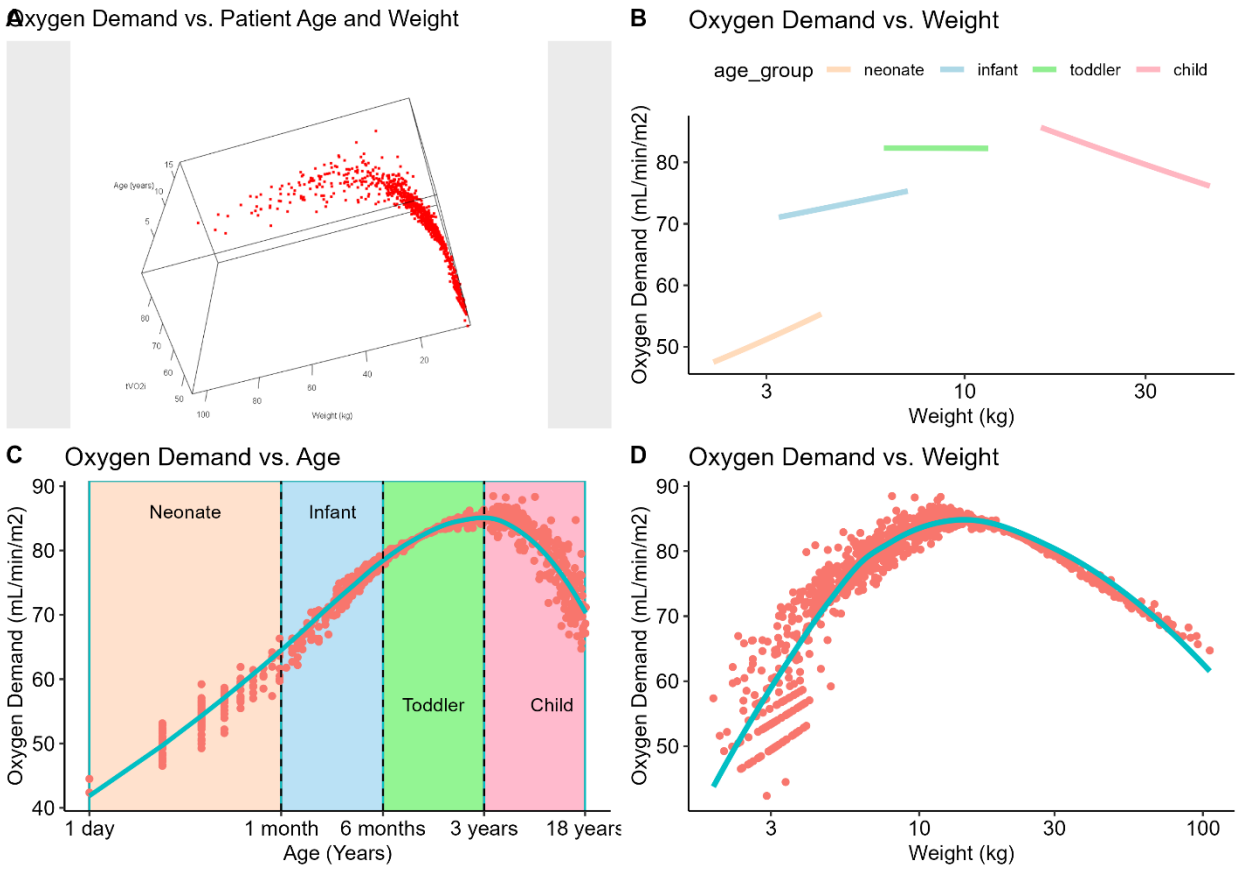

Figure 2: A) Oxygen demand ( ) vs patient age and weight, evaluated at (age, weight) pairs for patients in our data. B) Oxygen demand vs. weight at four different ages each representing an age group (neonate: 5 days, infant: 3 months, toddler: 1 year, child: 8 years). All oxygen demand numbers are calculated at a temperature of 35C using an augmented GARIX+(7) model. C) Projection of points in A onto the age- plane. Green line is a nonparametric (loess) regression of on age. Colour-shared areas represent neonate (orange), infant (blue), toddler (green) and child (pink) age groups. D) Projection of points in A onto the weight- plane.

Figure 3. OER Dynamics by Age group

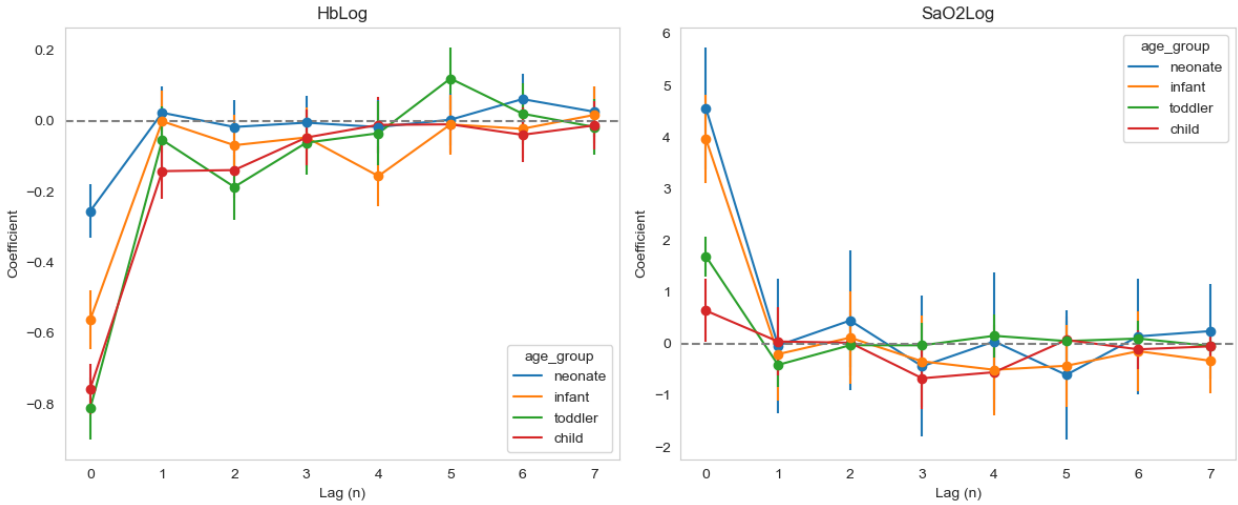

Figure 3: Coefficients of change terms in GARIX+ model involving haemoglobin (, left) and arterial oxygen saturation (, right), as a function of lag (n). Each colour corresponds to an augmented GARIX+(7) model that is trained on a subset of patients in a single age group. See Methods for exact definitions of change terms, lag and age groups.

Figure 4. Oxygen Demand vs. Temperature

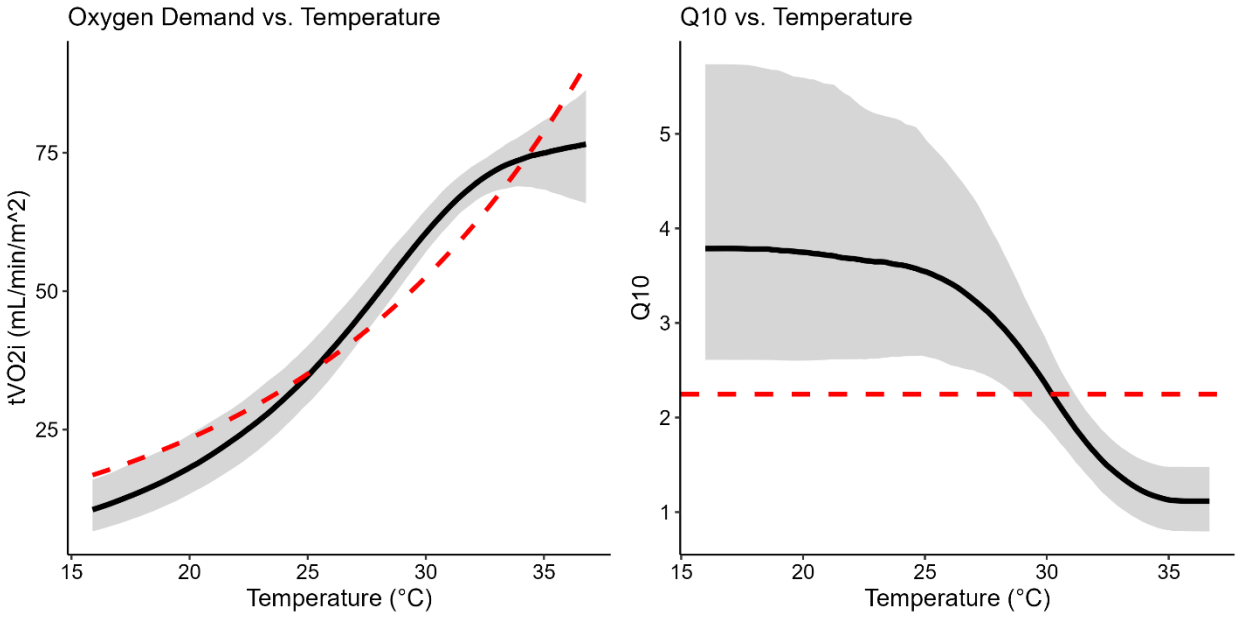

Figure 4: Oxygen Demand vs. Temperature. A: Estimated oxygen demand vs. temperature, with each point being the geometric average of the predicted values (by augmented GARIX+) for the unique (age, weight) combinations in training data. B:

Estimated Q10 vs. temperature, with each point being the arithmetic average of Q10 values for each (age, weight) pair in the data. Grey regions represent 95% confidence bands, using 1000 bootstrapped samples. Dashed red lines represent predictions from the baseline GARIX+(7) model.

Figure 5. GARIX+ vs. Fox82

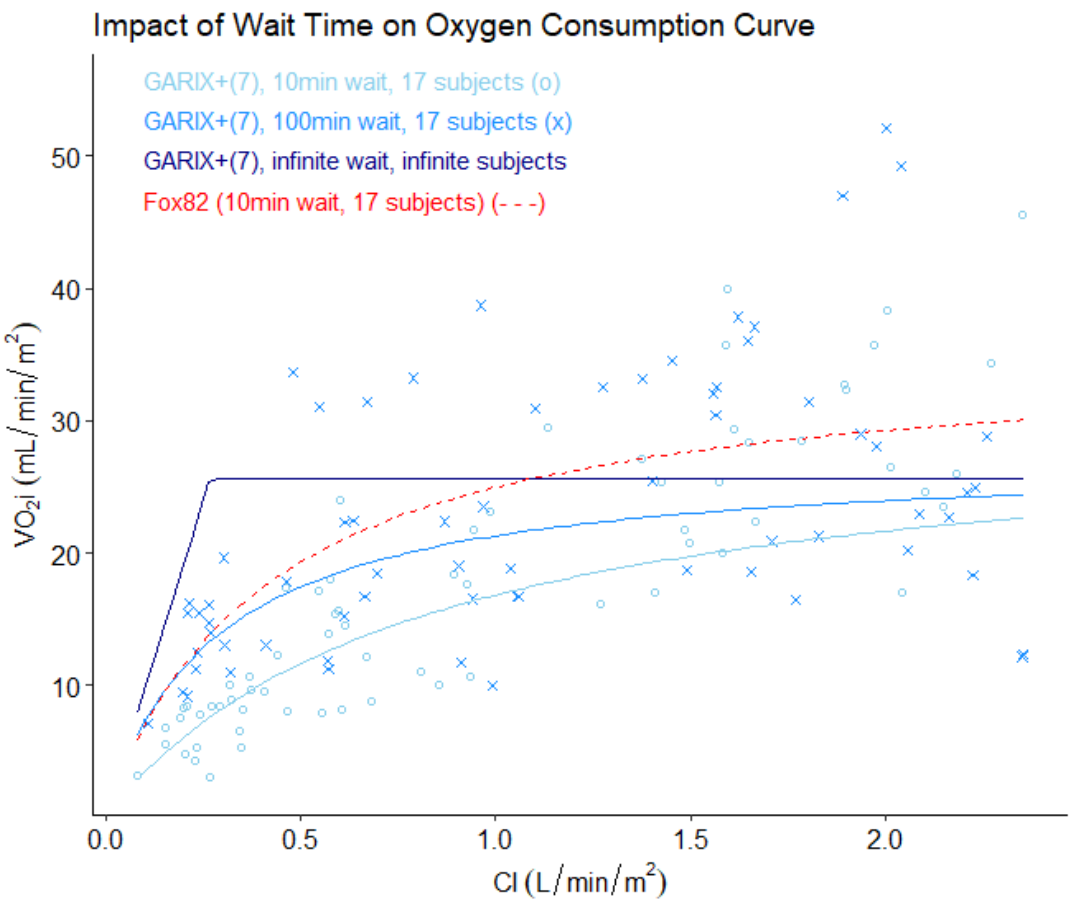

Figure 5: Comparison of VO2i vs. CI curves, produced by the baseline GARIX+ model (simulation-based) and the hyperbolic model of Fox82 (human experiments). Light blue ‘o’ marks show results of a sample stochastic simulation using GARIX+(7), with settings that closely match Fox82 (see Supp Mat B), including 17 subjects and a 10-minute wait after each step change to the CI. Light blue curve is the hyperbolic fit to simulated data. Blue ‘x’ marks are GARIX+(7) stochastic simulations using wait times of 100 minutes. The blue curve shows the hyperbolic fit to that data. The dark blue, piecewise linear line shows the results for infinite wait time and averaging over an infinite pool of (simulated) subjects. Dotted red curve is the hyperbolic fit of Fox82 to their human experiments.

Figure 6. Short-Term vs. Long-Term Oxygenation Gap

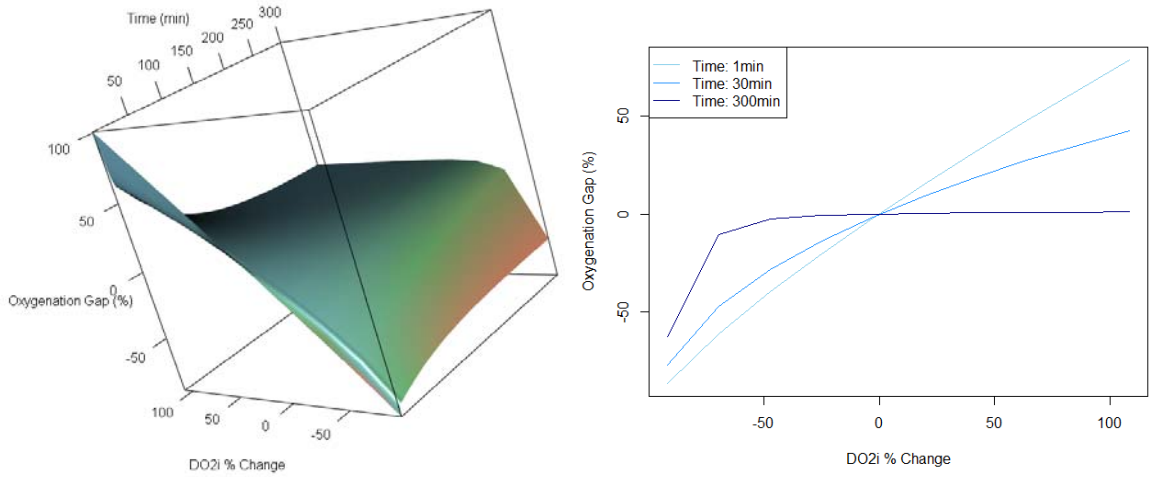

Figure 6: Short-Term vs. Long-Term Oxygenation Gap (OG). Oxygenation gap (OG) as a function of % change in DO2i (via a step change in CI at t = 0), at different wait times, using deterministic simulation with a baseline GARIX+ model. State variables are log(CI) = 0.217, log(Hb) = 1.96, log(SaO2) = 4.6, temp = 20, logit(OER) = -1.42. Positive OGs indicate over-oxygenation and negative OGs reflect under-oxygenation. See text for exact definitions.

Supplementary Materials

A: Nonstandard Abbreviations and Acronyms

- AKI: acute kidney injury
- ATG: autoregressive term group
- BSA: body surface area (m^2)
- CI: cardiac index (blood flow indexed to BSA; $L/min/m^2$)
- CPB: cardiopulmonary bypass
- CV: cross-validation
- DHCA: deep hypothermic circulatory arrest
- DO_2: oxygen delivery (mL/min)
- DO_2i: oxygen delivery, indexed to BSA ($mL/min/m^2$)

- EHR: electronic health record
- ETG: equilibrium term group
- GARIX: global autoregressive integrated (time-series model) with exogenous variables
- GARIX+: GARIX model, plus a disequilibrium term group (in addition to autoregressive and exogenous term groups)
- GDP: goal-directed perfusion
- Hb: haemoglobin content of blood (g/dL)
- i.i.d: independent and identically distributed
- ML: machine learning
- NICOR: national institute for cardiovascular outcomes research
- OER: oxygen extraction ratio
- OG: oxygenation gap
- OOS: out-of-sample
- PaO_2: partial pressure of oxygen (kPa)
- PRAiS2: partial risk adjustment in surgery model
- PVI: permutation-based variable importance
- Q10: multiplicative increase in the resting metabolic rate for every 10℃ increase in body temperature
- RBCs: red blood cells
- RMR: resting metabolic rate
- RTO: return-to-equilibrium (an estimated parameter in the GARIX+ model)
- SaO_2: oxygen saturation of arterial blood (%)

- SvO_2: oxygen saturation of mixed venous blood (%)
- TG: term group
- tVO_2i: target (indexed) oxygen consumption (indexed oxygen demand; mL/min/m^2)
- tDO_2i: threshold (indexed) oxygen delivery (mL/min/m^2)
- VI: variable importance
- VO_2: oxygen consumption (mL/min)
- VO_2i: oxygen consumption, indexed to BSA (mL/min/m^2)
- XTG: Exogenous Term Group

B: Methods

Study Design and Participants

Cohort is a retrospective analysis of consecutive patients aged younger than 18 years (maximum age treated at the institution) undergoing 963 CPB surgeries at Great Ormond Street Hospital between 2019 and 2021. Clinical data were collated in a research platform within the hospital's governance structure and de-identified before analysis. Institutional approval was given for the undertaking of this project (audit number 3045). Individual consent was not required because only routinely collected de-identified hospital data were evaluated within a secure digital research environment as part of an existing research database approval (17/LO/0008).

Data Collection

Routine clinical information was extracted from the institution's Electronic Health Record (EHR) system using a custom structured query language script. These data included demographic information, laboratory results, intraoperative, CPB, and medication administration data, and intensive care requirements. Comorbidities (including risk scores), and outcomes were defined using Association for European Paediatric and Congenital Cardiology coding as part of the institution's routine NICOR data submissions. Intraoperative data from the heart-lung and anaesthetic machines were captured every minute throughout surgery. Preoperative risk estimation was based on cardiac and non-cardiac preoperative risk factors using the Partial Risk Adjustment in Surgery (PRAiS2) model [7]. Baseline serum creatinine levels were taken within the 24 hours preceding surgery. Intraoperative blood biochemistry (including haemoglobin,

arterial oxygen partial pressure and saturation, and mixed-venous oxygen saturation) was measured continuously using an optical fluorescence and reflectance system (CDI550, Terumo, Leuven, Belgium), calibrated every 20 minutes using a cassette-based blood gas analyser (ABL90 Flex Plus, Radiometer, Copenhagen, Denmark). HLM variables were automatically recorded in one-minute intervals via a bidirectional connection into the Institutional EHR system (Axon, Philips Capsule, Paris, France). Postoperative AKI was calculated according to the Kidney Disease Improving Global Outcomes (KDIGO) criteria based on the patients' serum creatinine change and urine levels within the first 48 hours following surgery [8]. Patients were assigned the highest AKI grouping on the basis of these two criteria. The final KDIGO score for each patient is an integer between 0 (no AKI) and 3 (severe AKI).

Anaesthesia

Anaesthesia was induced by inhalation of sevoflurane in oxygen and, after induction, fentanyl 5 mg/kg and pancuronium100 mg/kg were given; maintenance was with isoflurane 1.0% in oxygen and air. After tracheal intubation, arterial and central venous lines were inserted. Further incremental doses of fentanyl, up to 25 mg/kg, were given during the procedure.

CPB

The CPB circuit consisted of FX oxygenators with integrated arterial line filter and hard-shell venous reservoir (Terumo). The St□cket S5 (St□cket, LivaNova, Munich, Germany) heart-lung machine with pole-mounted roller pumps was used with a 3T heater-cooler (St□cket). The total base prime volume was 330 - 1000 mL depending on circuit size. When the predicted initial CPB haematocrit was <27% the prime consisted of packed red blood cells of the patient's blood group (120-200mL), human albumin solution (50-150mL), heparin 1000 U/mL, 1.5 mL (Heparin Sodium; Wockhart, Wrexham, UK). Blood primed circuits were then washed with 1000 mL of balanced crystalloid solution (Plasmalyte 7.4; Baxter, Thetford, UK) by performing prebypass ultrafiltration, carried out as previously described, to ensure an initial on-CPB haematocrit of 30% [9]. Biochemical compatibility was then attained using sodium bicarbonate as a buffering agent. Patients requiring a clear prime received crystalloid and human albumin solution, with 10 mL sodium bicarbonate and 2 to 5 mL heparin. Myocardial protection was achieved with 30 mL/kg of cold blood cardioplegia (4:1 blood: cardioplegia to a final potassium concentration of 20 mmol/L) of St Thomas's Solution (IVEX Pharmaceuticals, Larne, Northern Ireland). During the rewarming phase of CPB, a gradient no greater than 10°C between the patient's oesophageal temperature probe and the heater-cooler (maximum arterial blood temperature 37.5°C) was maintained until a maximum oesophageal temperature of 36°C was achieved.

C: Fox82 Human Experiments and the Kirklin Equation

In this section, we briefly describe the experimental setup of Fox82 as well their synthesis of the human experiments they conducted along with previous experiments on animals. For details, see Fox et al (1982).

Fox82 Experiments

A total of 17 adults (15 males, 2 females) were included whose age was 57+/-10 years (mean +/- std). Mean body temperature during recordings was 21.3C. Initial CI was 2.2 L/min/m2. Mean venous Hb was 7.1. SaO_2 was not given, but we assumed a value of 99%, consistent with their assertion that 100% oxygen (no CO2) was used for ventilator oxygenation. After an initial stabilisation period, a randomly-shuffled sequence of five nominal CI's (0.25, 0.5, 1.0, 1.5 and 2.0 L/min/m2) were used with each patient, holding each level for 10 minutes. After device recalibration, actual flows were estimated to be 0.25 +/- 0.084, 0.54 +/- 0.101, 1.02 +/- 0.107, 1.56 +/- 0.129 and 2.08 +/- 0.180. We used these mean and std values to draw CI's for our simulations. Due to surgical constraints, the average number of 10-min episodes used with each patient was 4 (rather than 5).

Kirklin Equation

Kirklin et al (2012) combine the hyperbolic expression for the dependence of oxygen consumption on cardiac flow with the van't Hoff expression for the dependence of oxygen demand on temperature to arrive at the following equation for oxygen consumption (VO_2i) as a function of cardiac index (CI) and temperature (T):

$$\frac{1}{VO_2i} = 0.168 \times 10^{-0.0387\,T} + \frac{0.0378}{CI} \times 10^{-0.0253\,T} \qquad \text{(B.1)}$$

The numbers are based on fitting the equation to the human experiments of Fox82 done at 20C with the animal experiments of done at 37C. Equation B.1 implies a Q_{10} for oxygen demand (asymptotic oxygen consumption at infinite CI) of 2.4.

Evaluating the above equation at $T = 20$ produces the following hyperbolic equation, which is what Fox82 reported in their paper:

$$VO_2i = 35 \times CI \,/\, (0.42 + CI) \qquad \text{(B.2)}$$

D: OER Dynamics by Age Group – Remaining Variables

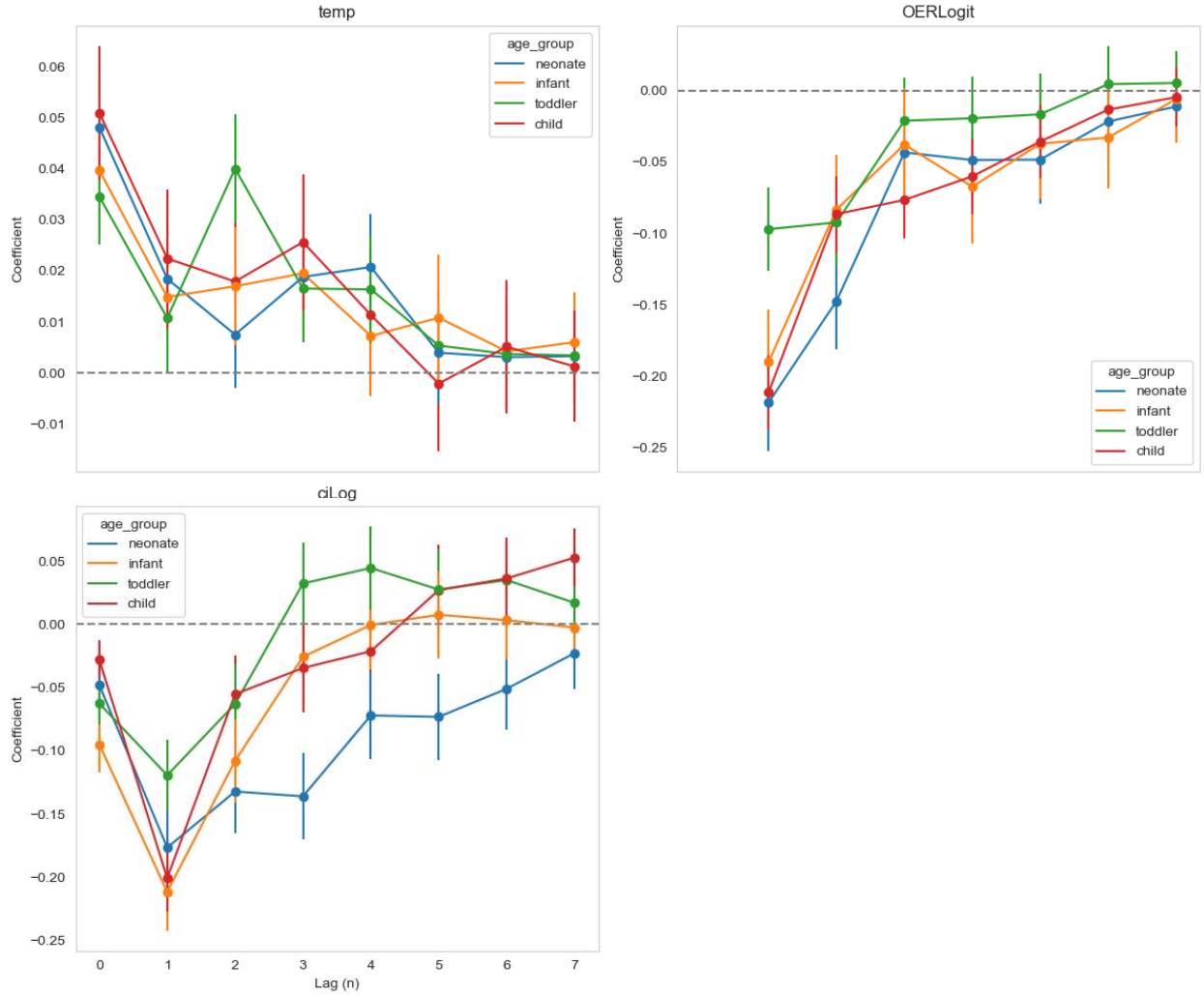

Figure D.1: Coefficients of change terms – as a function of lag (n) – in augmented GARIX+ for T, $logit(OER)$ and $\log CI$, stratified by age group.